# Title of your Senior Thesis or Junior Paper

Your Full Name

A Senior Thesis or Junior Paper
Presented to the Faculty
of Princeton University
in Candidacy for the Degree
of Bachelor of Arts

Recommended for Acceptance
by the Department of
Geosciences
Adviser: Your Adviser's Full Name

Date of Submission

*This paper represents my own work in accordance with University regulations,*

Your Signature

# Abstract

Your abstract should be less than 250 words and contain no references. The abstract should summarize objectives, methods, results, and conclusions

# Acknowledgements

Thank you to the following funding sources, my adviser, people who helped me with this study, read my proposals and thesis drafts, etc.

# Contents

# List of Figures

# List of Tables

# Introduction

The introduction should convey the purpose and scope of your study. The introduction also is where you include relevant background text and figures that give the reader the necessary context to understand the importance and meaning of your study. For example, the introduction might contain a map (Fig. 1) depicting sample locations.

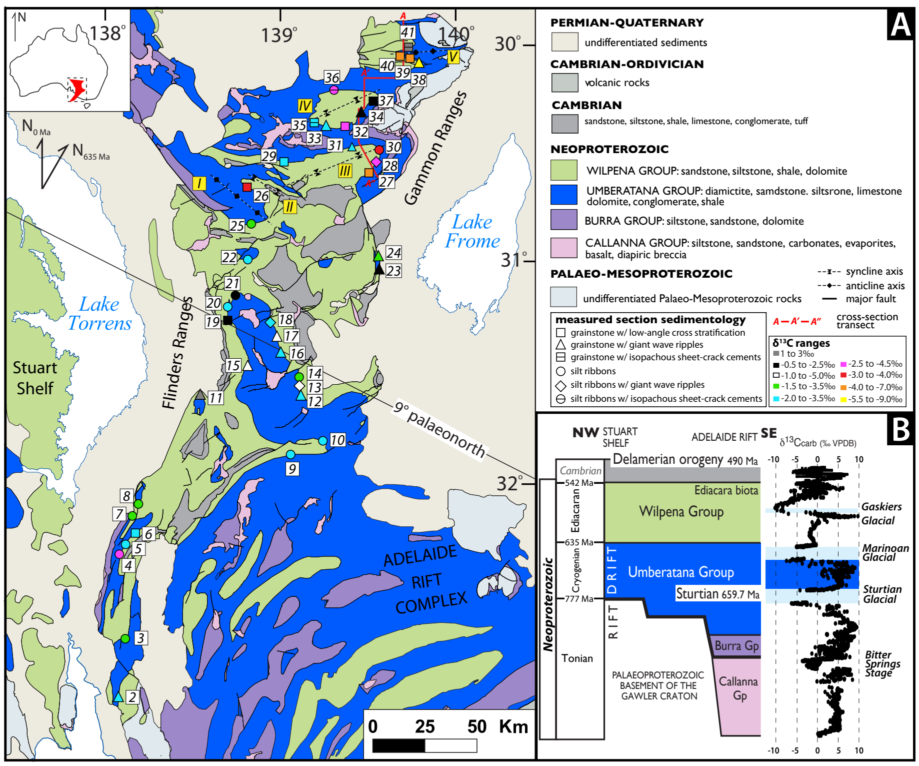


Figure 1: (a) Simplified geological map (adapted from **?**)) of the study area within the Adelaide Rift Complex (ARC). Locations of measured stratigraphic sections are denoted by red circles and labeled with numbered squares. (b) Schematic NW-SE stratigraphic cross-section of the Adelaide Rift Complex, highlighting the rift-to-drift transition and major sequence boundaries and U-Pb zircon ages. The $\delta^{13}C_{carb}$ profile (adapted from **?**) is time-aligned with the right-hand edge of the stratigraphic cross-section.

# Methods

The methods section should describe how you conducted field work, how you collected samples, how you designed lab work, what analytical methods you employed, etc. For example, if you collected GPS data, you would describe what type of electronics you used, how you designed your sampling, and how you measured the accuracy of individual measurements. You would accompany this information with a table or graph depicting, for example, the reproducibility of GPS measurements from identical physical locations at different times.

As another example, if you were modeling the strontium cycle in the ocean with the following mass balance equations, you could explain where these equations come from, and include Table (1) to collect information about the model variables.

$$\frac{dMg}{dt} = W_{Mg-carb} + W_{Mg-sil} - H_{Mg-clays} - P_{Mg-carb} \quad (1)$$

$$\frac{dCa}{dt} = W_{Ca-carb} + W_{Ca-sil} + H_{Ca-basalt} - P_{Ca-carb} \quad (2)$$

$$\frac{d^nSr}{dt} = W_{^nSr-carb} + W_{^nSr-sil} + H_{^nSr-basalt} - P_{^nSr-carb}, \quad (3)$$

| Model Variable | | | |
|---|---|---|---|
| weathering | | hydrothermal | |
| $W_{Mg-carb}$ | $2.0\times10^{12}$ mol/yr[1] | $k$ | $3.75\times10^{13}$ kg $H_2O$/yr |
| $W_{Ca-carb}$ | $10.5\times10^{12}$ mol/yr[1] | $H_{Mg-clays}$ | $k \cdot [Mg]$ |
| $W_{total_{Sr-carb}}$ | $1.1\times10^{10}$ mol/yr[2] | $H_{total_{Sr-basalt}}$ | $\alpha_{Sr/Ca} \cdot H_{Ca-basalt}$ |
| $W_{Mg-sil}$ | $4.0\times10^{12}$ mol/yr[1] | $\alpha_{Mg/Ca}$ | 1[4] |
| $W_{Ca-sil}$ | $4.5\times10^{12}$ mol/yr[1] | $\alpha_{Sr/Ca}$ | 0.0012[5] |
| $W_{total_{Sr-sil}}$ | $0.8\times10^{10}$ mol yr[2] | | |
| $^{87}Sr/^{86}Sr$ | | precipitation | |
| $W_{^{87/86}Sr-sil}$ | 0.7200[2] | $P_{Ca-carb}$ | $8.75\times10^{12}$ mol/yr[6] |
| $W_{^{87/86}Sr-carb}$ | 0.7075[2] | $P_{Mg-carb}$ | $1.6\times10^{12}$ mol/yr[7] |
| $H_{^{87/86}Sr-basalt}$ | 0.7030[2] | $P_{total_{Sr-carb}}$ | $(Sr/Ca)_{seawater} \cdot K_{Sr} \cdot P_{Ca-carb}$ |
| | | $K_{Sr}$ | 0.2[8] |

Table 1: Variables used in the numerical model of Mg, Ca, and Sr. [1]**?**; [2]**?**; [3]flux of $H_2O$ in hydrothermal systems assuming 100% of the heat flux at 350°C (**?**); [4]assumes 1:1 stoichiometry between Mg uptake and Ca release during basalt alteration; [5]calculated assuming 200 ppm Sr and 10 wt% CaO; [6]calculated assuming carbonate minerals are the only alkalinity sink; [7]estimated from the long-term rate of dolomitization (**?**); [8]homogeneous distribution coefficient for Sr in calcite (**?**).

# Results

This section will contain the bulk of your tables and figures, describing and illustrating the data you collected for your project. Do not interpret your data in the Results section. For example, let's say you collected information about the minimum ejecta thickness around a $\sim$2 km diameter bolide impact crater in India. You could collect those results in a figure like Fig. 2. However, you would avoid discussing the significance and meaning of these results until the Discussion section.

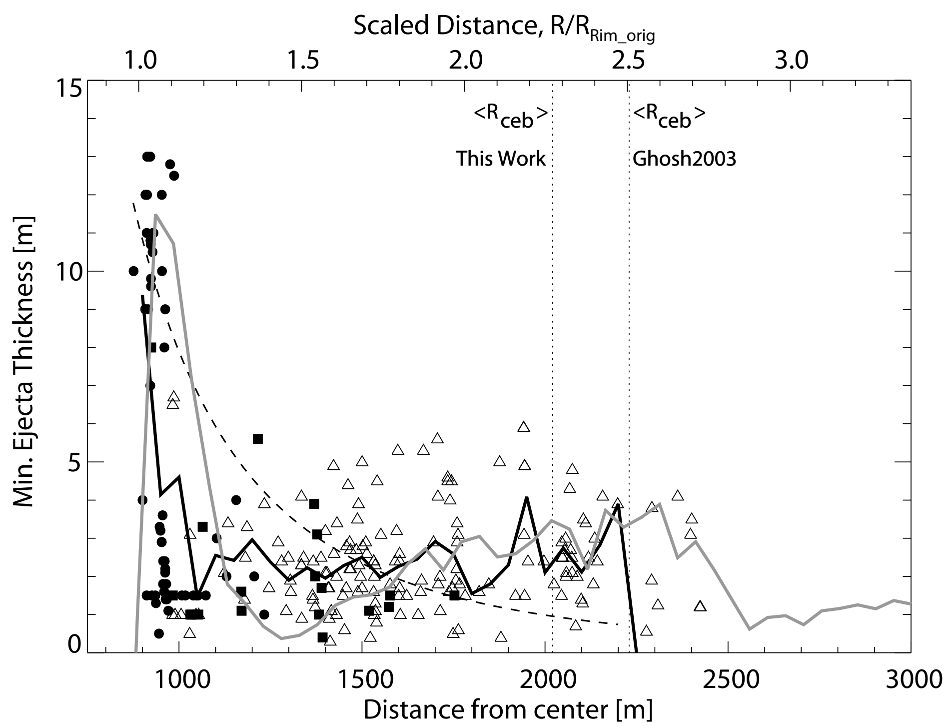


Figure 2: Minimum ejecta thickness measurements (circles-rim fold; squares-large blocks; triangles-small clasts at Lonar Crater, India. Average Lonar ejecta thickness profile (solid line) is compared to a ballistic ejecta thickness from experimental craters (dashed line **?**) and the topographic profile for a typical fresh Martian crater (grey line, scaled to Earth **?**). $R_{ceb}$ denotes the average extent of the continuous ejecta blanket (vertical dotted lines). Note the accumulation of ejecta amounting to ~5 times ballistic predictions at the distal edge of continuous ejecta blanket.

# Discussion

The Discussion section is where you have the chance to interpret the results you just reported on. Additional figures to illustrate your interpretations are useful. For example, you might compile your data with data from other sources to challenge existing hypotheses or generate new big-picture ideas.

So at this point we might sum up the main findings with a summary figure, for instance, as follows from **?**. Fig. 3 shows the large-$l$ variance ratio $(\sigma^2_\infty)^{\mathrm{MT}}$ plotted versus the bandwidths $0 \leq L \leq 20$ for single polar caps of various radii $0^\circ \leq \Theta \leq 180^\circ$ and double polar caps of various radii $0^\circ \leq \Theta \leq 90^\circ$. In the degenerate case $L = 0$, bandlimited 'multitaper' estimation is tantamount to whole-sphere estimation so $(\sigma^2_\infty)^{\mathrm{MT}} = 1$ regardless of the 'cap' size $\Theta$. Indeed, in that case, the estimate is unbiased, $M_{ll'} = \delta_{ll'}$, and at $L = 0$, the single possible taper is a constant over the entire sphere. For sufficiently large regions ($\Theta \gtrsim 30^\circ$ for a single cap and $\Theta \gtrsim 15^\circ$ for a double cap) the large-$l$ variance ratio is a monotonically decreasing function of the bandwidth $L$; for smaller regions the ratio attains a maximum value $(\sigma^2_\infty)^{\mathrm{MT}} > 1$ before decreasing. The grey curves are isolines of fixed Shannon number $K = (A/4\pi)(L+1)^2$; it is noteworthy that the $K = 1$ isoline passes roughly through the maxima of $(\sigma^2_\infty)^{\mathrm{MT}}$, so that for $K \geq 2$–$3$ the variance ratio is a decreasing function of the bandwidth $L$ regardless of the cap size. Since $K$ is the number of retained tapers, it will always be greater than 2–3 in a realistic multitaper analysis. For large Shannon numbers, above $K \approx 10$, the dependence upon the bandwidth $L$ and area $A$ for both a single or double cap can be approximated by the empirical relation $(\sigma^2_\infty)^{\mathrm{MT}} \approx (4\pi/A)^{0.88}/(2L+1)$. In particular, if $A = 4\pi$, the large-$l$ variance ratio is to a very good approximation equal to one divided by the number of adjacent degrees $l - L \leq l' \leq l + L$ that are averaged over by the coupling matrix $M_{ll'}$. As noted in Section , a whole-sphere multitaper estimate $\hat{S}^{\mathrm{MT}}_l$ can be regarded as a weighted linear combination of whole-sphere estimates of the form $\sum_{l'} M_{ll'} \hat{S}^{\mathrm{WS}}_{l'}$, so the variance is reduced by the number of independent random variates $\hat{S}^{\mathrm{WS}}_{l-L}, \ldots, \hat{S}^{\mathrm{WS}}_{l}, \ldots, \hat{S}^{\mathrm{WS}}_{l+L}$ that contribute to the estimate. For smaller regions of area $A \approx 4\pi$ the whole-sphere variance ratio $1/(2L+1)$ is empirically found to be increased by a factor $(4\pi/A)^{0.88}$. In fact, it is very

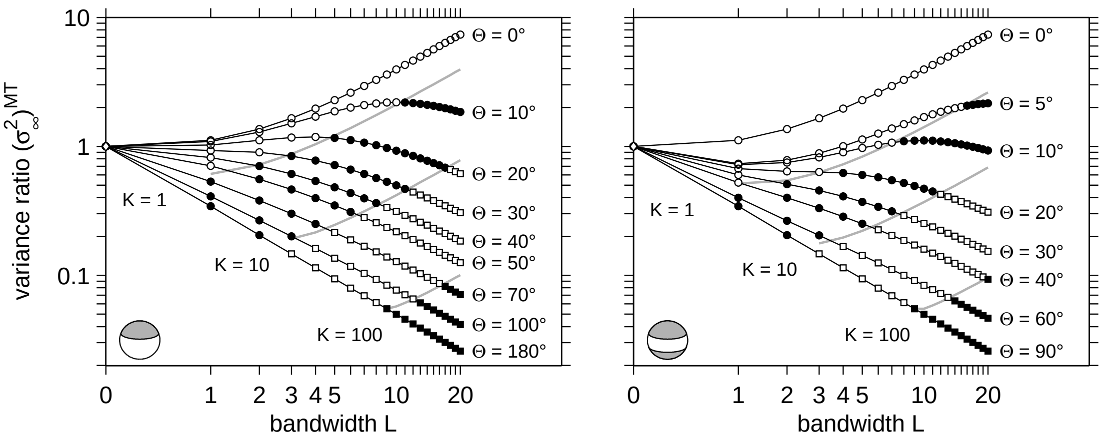


Figure 3: Variation of the large-$l$ multitaper variance ratio $(\sigma^2_\infty)^{\mathrm{MT}}$ with bandwidth $0 \le L \le 20$ for single polar caps of radii $\Theta = 0°, 10°, 20°, 30°, 40°, 50°, 70°, 100°, 180°$ (left) and double polar caps of common radii $\Theta = 0°, 5°, 10°, 20°, 30°, 40°, 60°, 90°$ (right). Ranges of the Shannon number $K = (A/4\pi)(L+1)^2$ are distinguished by different symbols: open circles $0 \le K \le 1$, closed circles $1 \le K \le 10$, open squares $10 \le K \le 100$, closed squares $K \ge 100$. Grey curves labeled $K = 1, 10, 100$ are Shannon number isolines. Axes are logarithmic to illustrate the $1/(2L+1)$ bandwidth scaling above $K \approx 10$.

reasonable to approximate the nearly-whole-sphere variance ratio at large Shannon numbers by $(\sigma_l^2)^{\mathrm{MT}} \approx (4\pi/A)^{0.88}(\sigma_l^2)^{\mathrm{MT}}_{A=4\pi}$ for all spherical harmonic degrees $0 \le l \le \infty$.

# Conclusions

Unlike the Results section (page 3), this section should be a clear statement of the major conclusions you have drawn from your work. The conclusions should follow clearly from the Results and Discussion sections.